International Journal of Applied Earth Observation and Geoinformation 152 (2026) 105453

Contents lists available at ScienceDirect

International Journal of Applied Earth Observation and Geoinformation

journal homepage: www.elsevier.com/locate/jag

The impacts of cover crop biomass on satellite-based detectability of cover crops in Maryland

Yide Xu[a,b], Qu Zhou[a,b,*], Kaiyu Guan[a,b,c,d,*], Sheng Wang[a,b], W. Dean Hively[e], Jyoti Jennewein[f], Alison Thieme[g], Steven Mirsky[h], Zhangliang Chen[a,b]

[a] Agroecosystem Sustainability Center, Institute for Sustainability, Energy, and Environment, University of Illinois Urbana-Champaign, Urbana, IL, USA
[b] Department of Natural Resources and Environmental Sciences, College of Agricultural, Consumer and Environmental Sciences, University of Illinois Urbana-Champaign, Urbana, IL, USA
[c] National Center for Supercomputing Applications, University of Illinois Urbana-Champaign, Urbana, IL, USA
[d] Siebel School of Computing and Data Science, University of Illinois Urbana-Champaign, Urbana, IL 61801, USA
[e] U.S. Geological Survey, Lower Mississippi-Gulf Water Science Center, Beltsville, MD, USA
[f] U.S. Department of Agriculture – Agricultural Research Service, Sustainable Agricultural Systems Laboratory, Fort Collins, CO, USA
[g] Department of Geographical Sciences, College of Behavioral and Social Sciences, University of Maryland College Park, College Park, MD, USA
[h] U.S. Department of Agriculture – Agricultural Research Service, Sustainable Agricultural Systems Laboratory, Beltsville, MD, USA

A R T I C L E I N F O

Keywords:
Cover cropping
Biomass
Management
HLS
Time series

A B S T R A C T

Cover crop adoption in the U.S. has increased over the past decades, increasing the need to quantify their performance and environmental benefits. While remote sensing (RS)-based approaches for detecting cover crop presence have been developed, there has been limited research on how cover crops with varied biomass and management practices influence detectability. Using unique field-level cover crop presence and biomass datasets in Maryland, U.S., we investigated how RS-based detectability changes for cover crops with varied aboveground biomass, planting, and termination dates. Specifically, we proposed a time-integrated satellite-based greenness feature from Harmonized Landsat-8 and Sentinel-2 (HLS) time series from 2017 to 2021 to estimate biomass of cover crops and evaluated their detectability using a phenology-based cover crop detection framework. The impacts of cover crop planting and termination dates on cover crop biomass were also analyzed. Our results demonstrated that Normalized Difference Vegetation Index (NDVI) estimated biomass with higher accuracy compared to other vegetation indices, and the time-integrated model estimated biomass with higher accuracy than the single-date "snapshot" linear model (R^2 from 0.53 to 0.66 and RMSE from 922 kg/ha to 747 kg/ha). While the snapshot models were species sensitive, the time-integrated models showed strong robustness across different species. Detectability increased with cover crop biomass, as detected cover crops averaged 963.3 ± 719.5 kg/ha compared to 297.2 ± 209.0 kg/ha for non-detected cover crops. Detection accuracy reached 96.1% for fields exceeding 500 kg/ha, compared with an overall accuracy of 62.7%. Earlier planting and later termination increased biomass and detectability, with biomass rising by 4.14 kg/ha/day ($p < 0.01$). This study demonstrates how management practices affect cover crop biomass and detectability via satellite time series and provides insights that can inform management of cover crops and monitoring of their effects on agroecosystems.

1. Introduction

Cover cropping is a common sustainable agriculture practice in many agroecosystems. The agroecological benefits that cover crops provide, such as soil conservation (Hu et al., 2023), weed control (Gerhards & Schappert, 2020), and climate adaptation (Delgado et al., 2021), are closely dictated by the amount of biomass they accumulate in their growing season. At low cover crop biomass (< 1000 kg/ha), cover crop residues prevent soil erosion (Prabhakara et al., 2015) but may have limited effects on physical and nutrient properties of soil in the long term (Ruis et al., 2020). Higher cover crop biomass (> 1000 kg/ha) enhances soil nitrogen retention (Hively et al., 2025), increases soil organic matter

* Corresponding authors at: Agroecosystem Sustainability Center, Institute for Sustainability, Energy, and Environment, University of Illinois Urbana-Champaign, Urbana, IL, USA.

E-mail addresses: quzhou2@illinois.edu (Q. Zhou), kaiyug@illinois.edu (K. Guan).

https://doi.org/10.1016/j.jag.2026.105453
Received 11 February 2026; Received in revised form 29 June 2026; Accepted 1 July 2026
Available online 15 July 2026

(Blanco-Canqui, 2022), and suppresses weed growth (Mirsky et al., 2013). However, high cover crop biomass is not always beneficial. For instance, several *meta*-analyses conducted in various contexts demonstrate that high cover crop biomass can decrease cash crop yield by competing for water and nutrients with cash crops (Abdalla et al., 2019; Lobell et al., 2025; Qin et al., 2021). Identifying cover crop practices and quantifying their biomass are essential steps in the evaluation of cover crop benefits in agroecosystems.

Satellite remote sensing is frequently used for monitoring crop growth. Various studies have implemented vegetation indices (VIs) derived from satellite remote sensing images to identify cover crops and estimate their biomass with machine learning and regression methods (Prabhakara et al., 2015; Chen, 2025; Zhou et al., 2026). However, existing studies typically address either site-scale biomass estimation or regional-scale cover-crop detection, and many require high-quality satellite data. Integrated approaches that simultaneously detect cover crops and quantify their biomass for monitoring remain scarce. Current detection methods use crop phenology, a factor that can be affected by biomass, to differentiate cover crops, cash crops, and weeds (Zhou et al., 2022; Ahmed et al., 2023). High cover crop biomass produces strong vegetation signals that can be confused with cash crops, whereas poor-performing cover crops are easily misclassified as weeds (Ahmed et al., 2023). Biomass variability remains an understudied yet critical factor influencing the accuracy of cover crop detection.

Remote sensing-based models for cover crop biomass estimation are typically developed from field data where cover crop presence is already known. Bridging the gap between cover crop detection and biomass estimation is critical for improving cover crop monitoring and assessing their agroecological impacts at large scales. VIs, such as Normalized Difference Vegetation Index (NDVI), Near-Infrared Reflectance of Vegetation (NIRv), Enhanced Vegetation Index (EVI), and Green Chlorophyll Vegetation Index (GCVI), have been used for crop biomass estimation (Prabhakara et al., 2015; Servia et al., 2022; Thieme et al., 2023; Cai et al., 2024; Liu et al., 2023). Modeling crop biomass from snapshot VIs is challenging because many indices saturate at high biomass, and VIs may have varied performance due to their different characteristics. Therefore, evaluation of these indices for cover crop biomass estimation is essential to understand how biomass affects cover crop detectability and to quantify the benefits of agroecosystems more accurately.

Cover crop biomass is influenced by environmental conditions and strongly affected by management strategies that further influence its remote sensing-based detectability. For example, farmers must decide when to plant and terminate their cover crops. A longer growing period provides more time for cover crops to accumulate biomass, which leads to greater biomass values (Thieme et al., 2023) and may therefore offer more ecological benefits (Mirsky et al., 2013). Quantitative analyses showed that fall-planted rye (*Secale cereale* L.) produced 57–74% more biomass compared to rye planted only 3–7 weeks later in early winter (Ruis et al., 2020), and delaying termination until the day of cash crop planting increased biomass by up to 146% compared to termination four weeks earlier (Kumar et al., 2025). However, planting cover crops too early may increase the risk of winterkill due to freezing temperatures (Fowler et al., 2014), and terminating cover crops too late may delay cash-crop planting and reduce yields (Lobell et al., 2025). Therefore, decisions on planting and termination dates affect both the cover crop biomass and its agroecological outcomes. Understanding how management practices modulate cover crop biomass supports recommendations for stakeholders to better manage their cover crops for optimal benefits.

Building on a previously developed cover crop detection approach (Zhou et al., 2022), this study aims to **investigate how cover crop biomass under different management practices affects its detectability by satellite remote sensing** and to **improve methods for cover crop management and monitoring.** To address the above-mentioned scientific gaps, we aim to answer the following questions: (1) How can we accurately estimate cover crop biomass for varied cover crop species from satellite data? (2) What are the impacts of biomass on satellite-based cover crop detection? (3) What are the impacts of cover crop management on cover crop biomass? To answer these questions, we first evaluated and compared the accuracies of several VIs, including NDVI, EVI, NIRv, and GCVI, in both single-date "snapshot" and time-integrated forms, for biomass estimation of cereal rye, wheat (*Triticum aestivum*), and triticale (×*Triticosecale*). Next, using the optimal biomass model, we quantified cover crop detection accuracy for different biomass levels using our previous detection framework. Finally, we analyzed cover crop biomass differences under varied planting and terminating dates to understand management impacts on cover crop biomass and detectability.

2. Study region and data

2.1. Study region

Our study was conducted in the State of Maryland, U.S. (Fig. 1). The Maryland cover crop initiatives aim to reduce erosion and nutrient loss, improve soil health, protect the Chesapeake Bay watershed, and support carbon sequestration. The state cover crop program offers incentives to farmers based on species, planting and termination timing, and seeding methods (Maryland Department of Agriculture, 2024). Eligible crops include wheat, cereal rye, triticale, barley (*Hordeum vulgare*), oats (*Avena sativa*), and ryegrass (*Lolium*); mixture options include brassicas such as forage radish (*Raphanus sativus*) and rape (*Brassica napus*), as well as legumes such as clover (*Trifolium* spp.) and winter peas (*Pisum sativum*). The program-specified planting dates vary by cover crop species and seeding methods: cereal grains before November 5th; oats and mixes containing legumes and brassicas before October 10th; aerial seeding before October 1st. The program also mandates termination dates between March 1st and June 1st.

2.2. Data

We utilized four major dataset categories in this study, including cover crop ground truth data (location and biomass), satellite time series data, environmental data, and auxiliary data (Supplementary Table 1).

For biomass modeling, we used in situ winter cover crop biomass data collected by the U.S. Geological Survey (USGS) and U.S. Department of Agriculture (USDA)-Agriculture Research Service (ARS) (Jennewein et al., 2022). A total of 327 biomass samples were collected from fields at the USDA-ARS Beltsville Agricultural Research Center (BARC), Beltsville, Maryland, USA (Fig. 1) during November–April for 2019–2021. The BARC data include biomass data from commonly planted cereal species, such as wheat, cereal rye, and triticale. The centroids (n = 16,635) of a subset (15%) of cover crop fields enrolled in the Maryland Department of Agriculture (MDA) cover crop program from 2017–2018 to 2020–2021 were used to validate our cover crop detection accuracy, along with a similar 15% subset of fields (n = 18,551) not enrolled in cover crop cost-share for each year. County-level cover crop acreages from the USDA National Agricultural Statistics Service (NASS) Quick Stats (USDA NASS 2017-2022) for the years 2017 and 2022 were used to constrain the detection framework.

We used the NASA Harmonized Landsat Sentinel-2 (HLS) (version 2) data covering Maryland from 2017 to 2024 to detect cover crop phenology. HLS combines the Landsat 8 and Sentinel-2 data, providing consistent surface reflectance products at 30-m and ~3-day resolutions (Claverie et al., 2018). The high-quality HLS time series were used to identify cover crop fields, estimate cover crop planting date and termination date, and model cover crop biomass. The HLS QA band was used to remove contaminated pixels such as clouds, cloud shadows, snow, or water.

The environmental data included 10-m gSSURGO (Gridded Soil Survey Geographic Database) soil data in 2020 (Soil Survey Staff, 2020), and 2.5-arc Parameter-elevation Regressions on Independent Slopes

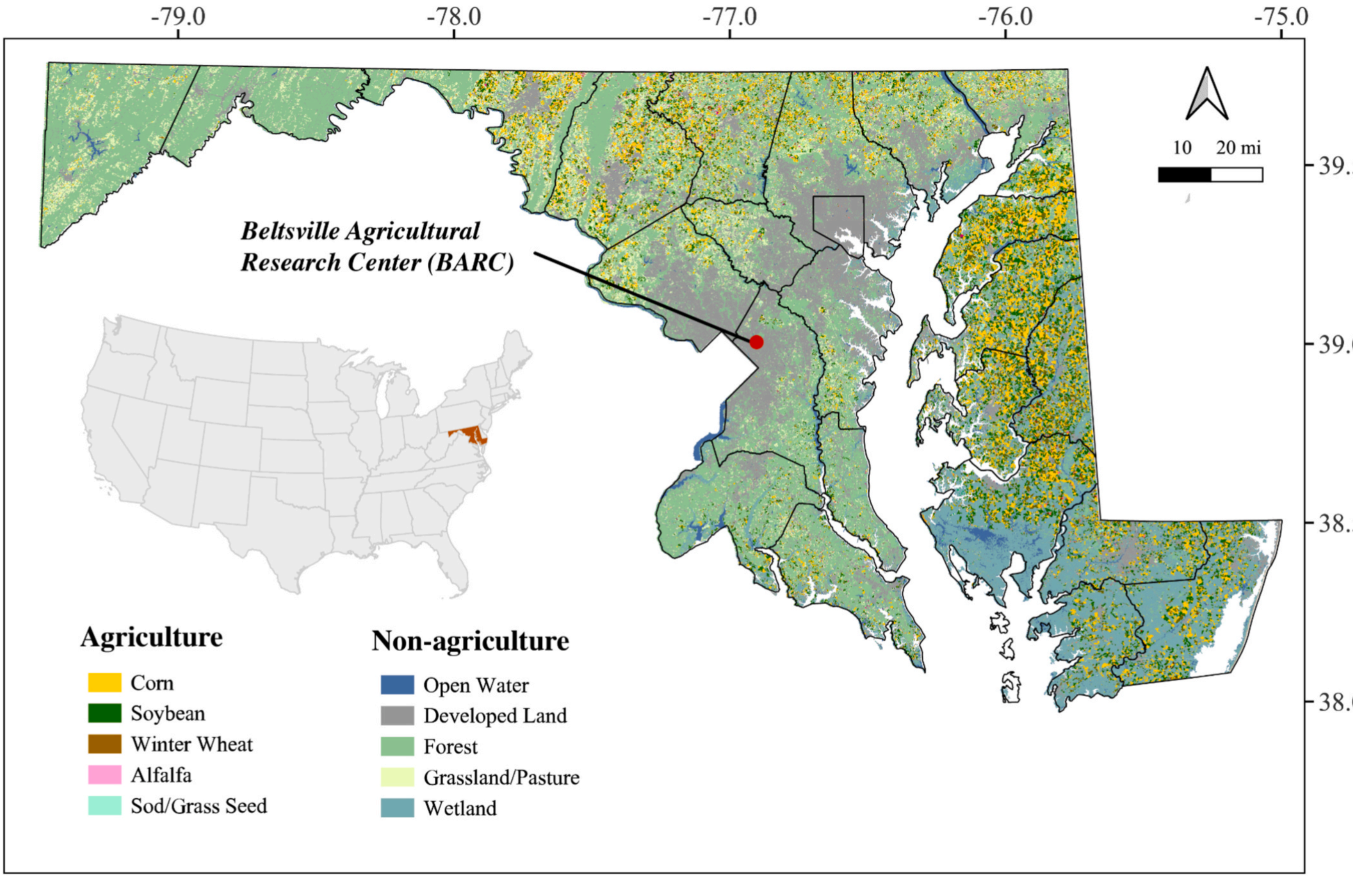

Fig. 1. Study area: Maryland. The figure shows the 2024 Cropland Data Layer (CDL) (Boryan et al., 2011) of Maryland. The legend shows some common land cover types in both the agriculture and non-agriculture categories. The map labels Beltsville Agricultural Research Center (BARC), where winter cover crop biomass data were collected.

Model (PRISM) climatic data from 2017 to 2022 (PRISM Climate Group, 2022). These environmental datasets were used in the cover crop detection framework.

The auxiliary data included the 30-m CDL (Boryan et al., 2011) and Crop Sequence Boundaries (CSB) (Abernethy et al., 2023). Both datasets were used to identify agricultural lands where cover crops could be planted.

3. Methods

We completed this study following three major steps (Fig. 2): (1) extracting vegetation indices and cover crop features using HLS time series, and using BARC biomass data to build the cover crop biomass model; (2) building the cover crop detection model based on cover crop feature, NASS county-level data, and environmental variables following our previous framework (Zhou et al., 2022), generating detected cover crop map, and validating the map using MDA cover crop data; (3) generating the cover crop biomass map by combining the detection map with the biomass model.

3.1. Extract time-integrated vegetation index

We selected four VIs (NDVI, EVI, NIRv, and GCVI) to test and compare their capacity to predict cover crop biomass using BARC data.

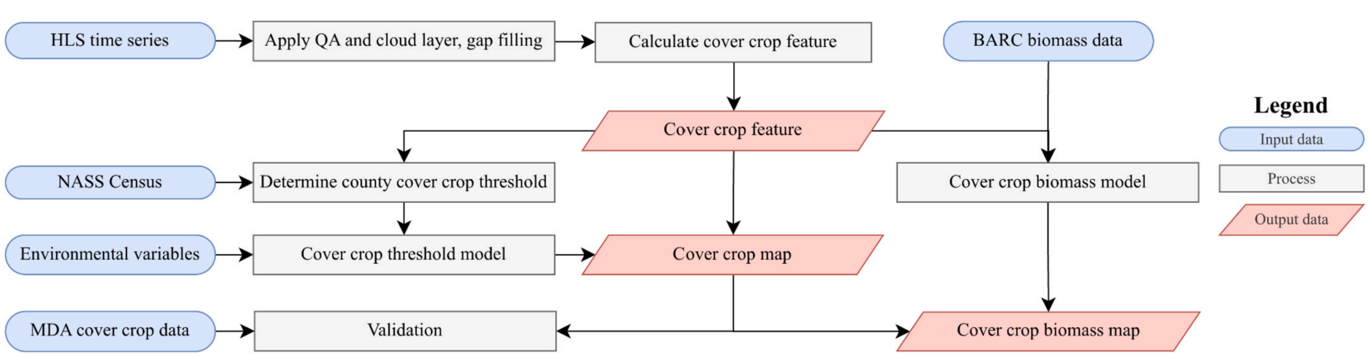

Fig. 2. Framework for mapping cover crop biomass. Snapshot and time-integrated VIs from HLS time series are used with BARC data to build the biomass model. A cover crop detection model is then developed using extracted features, NASS county-level data, and environmental variables following Zhou et al. (2022), and validated with MDA centroid data. Biomass maps are generated by integrating detection results with the biomass model, followed by analysis of spatiotemporal patterns, detection thresholds, and factors influencing biomass.

The selected VIs were related to vegetation physiology and have been utilized to monitor crop growth, yield, biomass (Fan et al., 2021; Shammi & Meng, 2021; Shuai et al., 2024), and cover crop performance (Hively et al., 2025; Thieme et al., 2023; Prabhakara et al., 2015). NDVI has primarily been used to quantify vegetation greenness and served as an indicator of vegetation density and plant health. EVI, like NDVI, can be used to quantify vegetation greenness and phenology. EVI is more sensitive in areas with dense vegetation and high biomass (Huete et al., 2002). NIRv tracks photosynthetic activity and gross primary productivity, and it can better isolate the vegetation signal by reducing the influence of soil background (Badgley et al., 2017). GCVI is sensitive to chlorophyll concentration and leaf nitrogen content, which are related to plant physiological status (Gitelson et al., 2003). The equations of these indices are

$$NDVI = \frac{NIR - Red}{NIR + Red} \tag{1}$$

$$EVI = \frac{NIR - Red}{NIR + 6 \cdot Red - 7.5 \cdot Blue + 1} \tag{2}$$

$$GCVI = \frac{NIR}{Green} - 1 \tag{3}$$

$$NIRv = NIR \cdot NDVI \tag{4}$$

To develop the time-integrated VI features, we modified the feature calculation method in the previously developed phenology-based cover crop detection framework (Zhou et al., 2022). VI time series of each pixel were collected. After filtering out abnormal VI values and interpolating missing values, we applied the Savitzky-Golay filter to smooth the time series. We extracted full-season features integrating VI signals across the entire winter, rather than focusing solely on spring greenness. The time-integrated VI feature (f) is given by the equation below,

$$f = \sum_{i=d_1}^{d_2} (index_i - index_{baseline}) \tag{5}$$

$$index_{baseline} = min(index_{d_1}, index_{d_2}) \tag{6}$$

where d_1 and d_2 were the dates when the lowest VIs were observed before the latest planting date and after the earliest termination date, respectively. Baseline $index_{baseline}$ was removed to minimize background influence, such as soil. Fig. 3 shows an example of the HLS NDVI time series of a cover crop field in the 2020–2021 season.

3.2. Cover crop biomass modeling

Cover crop biomass has a strong and positive log-linear correlation with field greenness (Thieme et al., 2023). We tested the performance of both the single-date snapshot and time-integrated VIs in predicting cover crop biomass using BARC data. Regression models were built for all and specific species using both snapshot (*index*) and time-integrated greenness index feature (f). Snapshot VIs were derived from the band values measured nearest to the termination date in the BARC biomass dataset. We applied natural logarithmic transformation to biomass and fit regression models (Prabhakara et al., 2015; Thieme et al., 2023). The following equations represent the models.

$$ln(Biomass) = a \cdot index + \epsilon_1 \tag{7}$$

$$ln(Biomass) = b \cdot f + \epsilon_2 \tag{8}$$

We then compared the performance of models using R^2 and the root mean square error (*RMSE*). The best model was used for cover crop biomass estimation in the following sections. We applied analysis of covariance (ANCOVA) to the biomass regression models to evaluate whether species differed in their regression parameters.

3.3. Cover crop detection

The detection framework was mainly adapted from the one developed by Zhou et al. (2022). When applied to Maryland, we expanded the feature date range to include the winter cover crop feature along with the spring feature and fall feature, if cover crop growth was observed in the fall. The previous feature version in Zhou et al. (2022) only used the cover crop spring feature, which did not capture the cover crop growth in both fall and winter. Assuming cover crops exhibit greater greenness than weeds, we established a greenness threshold to aid cover crop detection by distinguishing them from weeds. More details are in the Supplemental Materials.

The predicted cover crop map was finalized after applying a low-pass filter to remove speckling. We then used the centroids of 15% of MDA-enrolled cover crop fields and non-cover crop fields to validate the detection results for each year. Because the MDA data were point-based, we evaluated detection accuracy using two complementary criteria. First, we applied a proximity-based criterion in which an MDA ground truth point was considered correctly detected if it overlapped a predicted cover-crop pixel, or if at least one predicted cover-crop pixel

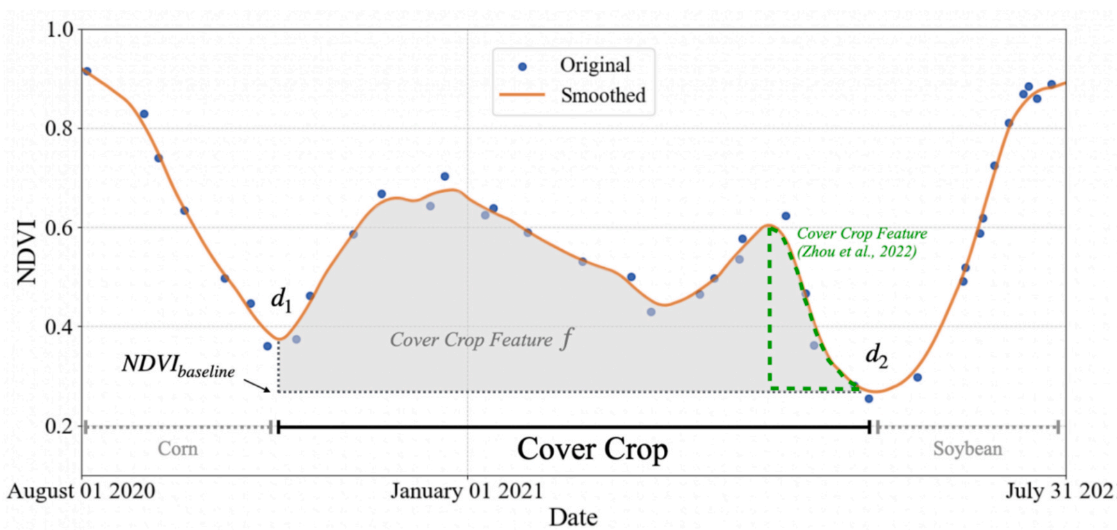

Fig. 3. Method to calculate the accumulated greenness index. The figure shows an HLS NDVI time series of a cover crop field planted in the season 2020–2021 in Kent County, MD. The cash crops before and after the cover crop season are corn and soybeans.

occurred within a one-pixel buffer (a 3x3 pixel window). Second, we conducted a majority-based assessment to account for spatial uncertainty in point locations and raster alignment. In this method, a detection was successful when the majority of pixels within the one-pixel buffer were classified as cover crops or non-cover crops.

3.4. Analyze the biomass patterns and influencing factors

Using biomass models and predicted cover crop maps, we estimated biomass for all MDA-enrolled fields and compared detected versus non-detected fields. We evaluated whether species affected detection rate and biomass using an ANOVA test. County- and year-level median biomass were calculated to examine spatial and temporal patterns across Maryland from 2017 to 2022, with emphasis on the Delmarva Peninsula, a major agricultural region. Using MDA records of enrolled cover crop fields, we analyzed the effect of management timing (growth time) and accumulated growing degree days (AccGDD) on biomass. AccGDD is calculated using a base temperature of 4 °C (Hively et al., 2025). To minimize bias from sparsely sampled extreme dates, we fitted Gaussian curves to sample-count distributions and excluded the outermost 2.5% of samples. The mean biomass of enrolled cover crop samples was calculated for 7-day planting and termination intervals and used in correlation analyses. We used AIC scores to determine linear or quadratic relationships between variables and biomass.

4. Results

4.1. Biomass modeling

Regarding cover crop biomass prediction, NDVI demonstrated higher accuracy compared with other VIs for both snapshot and time-integrated models, while time-integrated indices were more accurate than snapshot-based indices (Supplementary Table 4). Snapshot NDVI achieved a performance of $R^2 = 0.53$ and RMSE = 922 kg/ha, outcompeting other indices. NDVI outperformed other indices when used as a time-integrated form. Compared with snapshot NDVI, time-integrated NDVI showed improvements in terms of R^2 (0.53 to 0.66) and RMSE (922 kg/ha to 747 kg/ha) in predicting cover crop biomass. For both snapshot and time-integrated VIs, the saturation problem emerged for estimating high-biomass cover crops (Fig. 4). At high biomass levels (≈ 4000–8000 kg/ha), large variations in biomass corresponded to small changes in both snapshot and time-integrated NDVI.

Additionally, the time-integrated NDVI models were more robust in predicting cover crop biomass for triticale, cereal rye, and all-species models (Fig. 4). Models across species were similar when the time-integrated NDVI was used (ANCOVA p-value = 0.339). The snapshot NDVI models showed greater interspecies variation (ANCOVA p-value < 0.001), indicating recalibration may be needed when modeling biomass for new species. The reduced interspecies model variation achieved by adopting time-integrated NDVI suggested that a global biomass model could be developed for different species. The model was also insensitive to the baseline uncertainty. Our Monte Carlo simulation indicated that the baseline variation led to an uncertainty of 0.012 in R^2 for biomass estimation (Supplementary Fig. 3). Thus, we decided to use time-integrated NDVI to estimate cover crop biomass.

4.2. Cover crop biomass and detection

4.2.1. Cover crop feature threshold and detection

Statewide cover crop and non-cover crop detections were predicted with high accuracy during 2017–2020, with consistent accuracy during 2017–2019 across all validation criteria (Figs. 5–6). The accuracy improved by 9.6% compared to the previous feature calculation method under the proximity-based rule (Supplementary Table 3). Detection rates declined in 2020 under both proximity- and majority-based rules, likely due to reduced program enrollment following lower incentive payments and pandemic-related disruptions to verification, which increased uncertainty in ground-truth data (Gao et al., 2023). Detection accuracy also varied regionally. Eastern Maryland counties on the Delmarva Peninsula (Eastern Shore) had a higher and more stable cover crop detection rate than the western counties of Maryland (Fig. 5). Western counties had limited agricultural land and a small number of fields that were enrolled in the MDA cover crop program. Using the annual dataset of fields not enrolled in the cover crop program, results

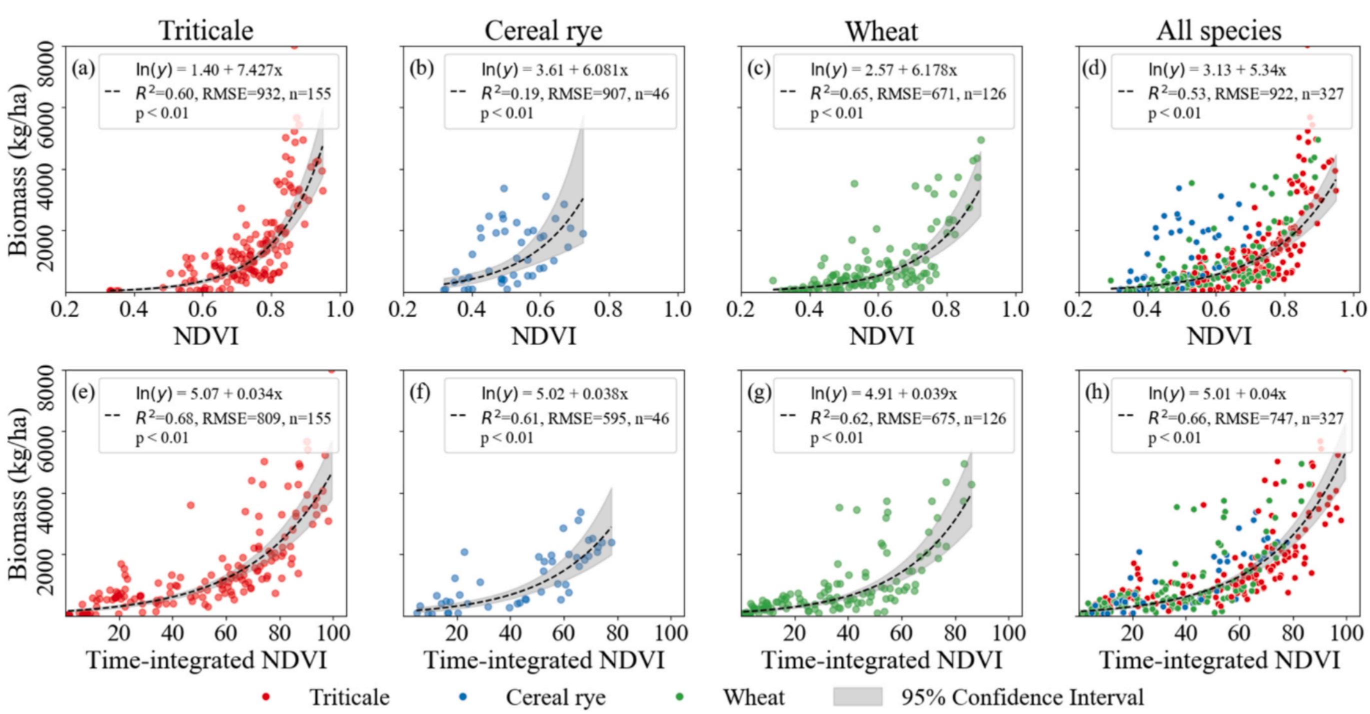

Fig. 4. Comparison of biomass prediction models across species using time-integrated and snapshot NDVI. Panels (a)–(d) present models based on snapshot NDVI. Panels (e)–(h) display models based on time-integrated NDVI cover crop features.

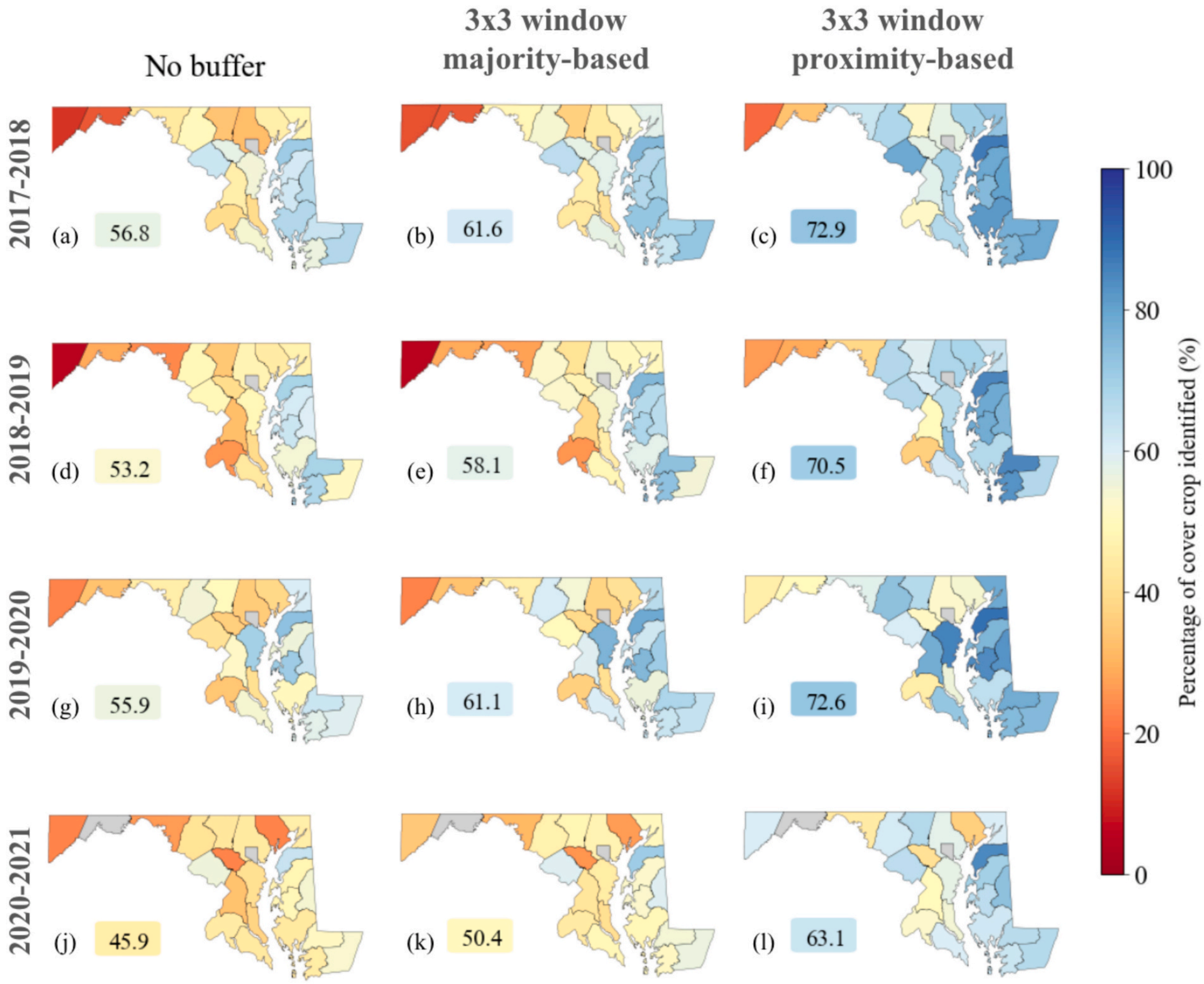

Fig. 5. County- and state-level accuracy of cover crop identification across years (rows) and detection criteria (columns). Labels in the lower-left side indicate the statewide identification rates (%). Gray color signifies no ground truth data.

showed that non-cover crop identification maintained high accuracy statewide under both rules, with commission errors lower in western counties (Fig. 6).

4.2.2. Temporal and spatial variation of detected and non-detected cover crop biomass

Detected cover crops had significantly higher estimated biomass than non-detected cover crops, a pattern consistent across years and locations. The difference in biomass distribution between the detected and non-detected cover crops (no buffer) was consistent for each year between 2017 and 2020 (Fig. 7a). Statewide, detected cover crops (963.3 ± 719.5 kg/ha) had higher estimated biomass than non-detected cover crops (297.2 ± 209.0 kg/ha) across all years (Fig. 7b). The overall detection accuracy was 62.7%, but the accuracy for fields that had estimated biomass exceeding 500 kg/ha was 96.1%. Based on Maryland samples, a biomass threshold of 361 kg/ha corresponded to > 90% probability of detection.

Cover crop biomass in Maryland spatially increased from the northwest to the southeast, likely demonstrating elevation and latitude constraints on cover crop growth. The county-level median biomass (Fig. 8) was highest in southern and Delmarva Peninsula counties, coinciding with the high detection accuracy from 2017 to 2020 (Fig. 5). Winter biomass values of 2019–2020, 2021–2022, and 2022–2023 seasons were greater compared to other years, potentially linked to high accumulated growing degree days (GDD) (Hively et al., 2025). The biomass dropped in 2020–2021 might be due to a combination of cold winter (Hively et al., 2025), insufficient incentives, and pandemic disruption. These spatial and interseasonal biomass variations highlighted the influence of environmental conditions on cover crop growth and demonstrated the utility of an adaptive cover crop feature threshold model.

On the Delmarva Peninsula, the cover crop biomass increased from north to south, and so did the gap between the biomass of detected and non-detected cover crops. Southern counties in the peninsula showed higher median biomass (Fig. 9). The combined 2017–2020 data indicated a significant negative relationship between biomass and latitude for both detected (p = 0.021) and non-detected fields (p = 0.043). Notably, the biomass of detected cover crops increased at a rate approximately six times greater than that of non-detected cover crops toward the southern counties. Conversely, the biomass gap narrowed at higher latitudes, indicating less differentiated detection performance in northern areas where overall biomass was lower.

4.2.3. Interspecies variation

High cover crop biomass led to higher detection accuracy, regardless of the cover crop species. Fig. 10 presents Maryland's most popular cover crop types, which are cereal rye, wheat, and barley. The general trend indicated that mean annual cover crop biomass of each species was significantly and positively related to detection accuracy ($p < 0.05$). The ANOVA test of accuracy among species showed F = 1.302, p = 0.319, suggesting that species did not significantly influence detection accuracy. Other cover crop functional types (e.g., legumes) were not

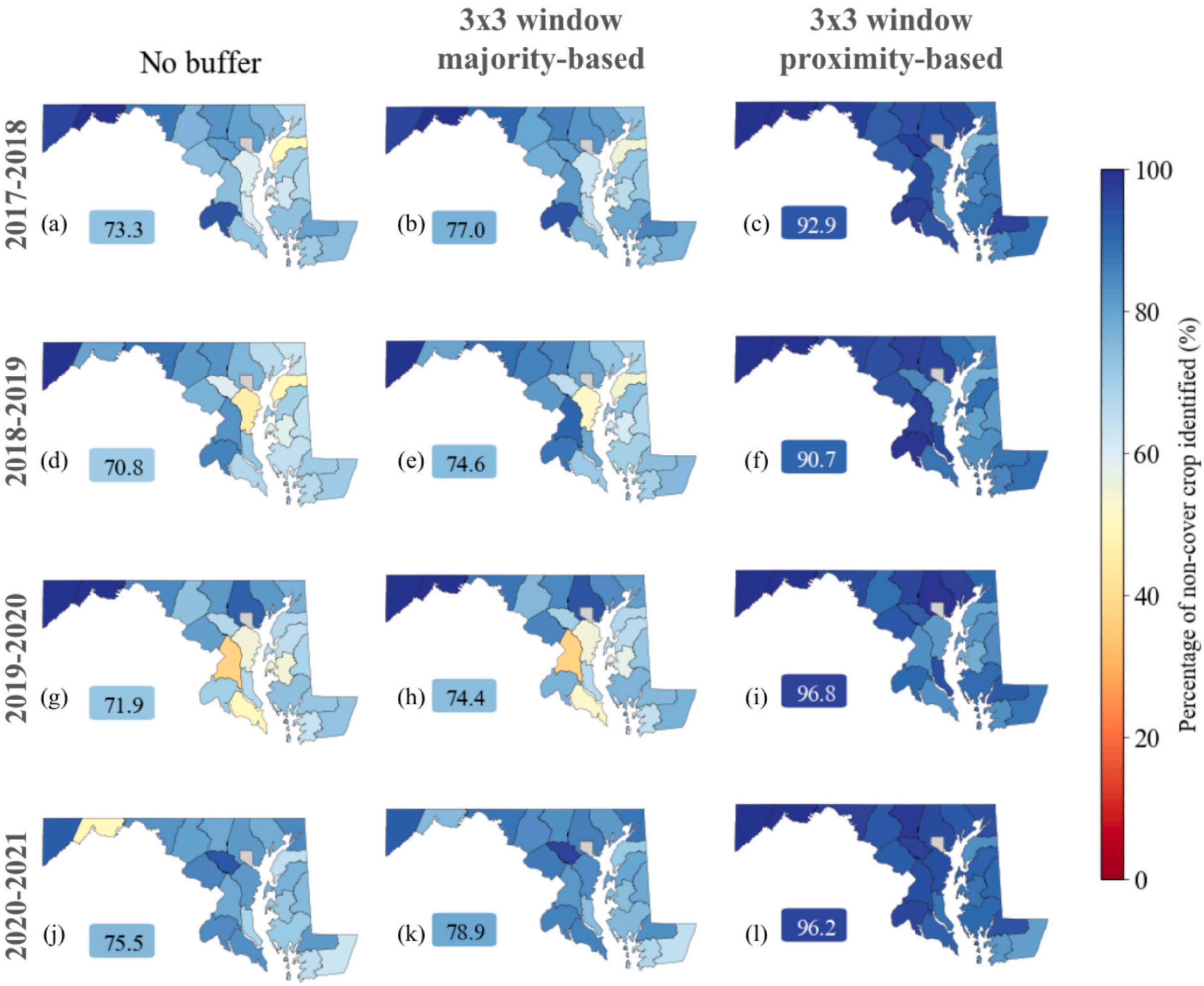

Fig. 6. County- and state-level accuracy of non-enrolled cover crop identification across years (rows) and detection criteria (columns). The layout is similar to the layout in Fig. 5.

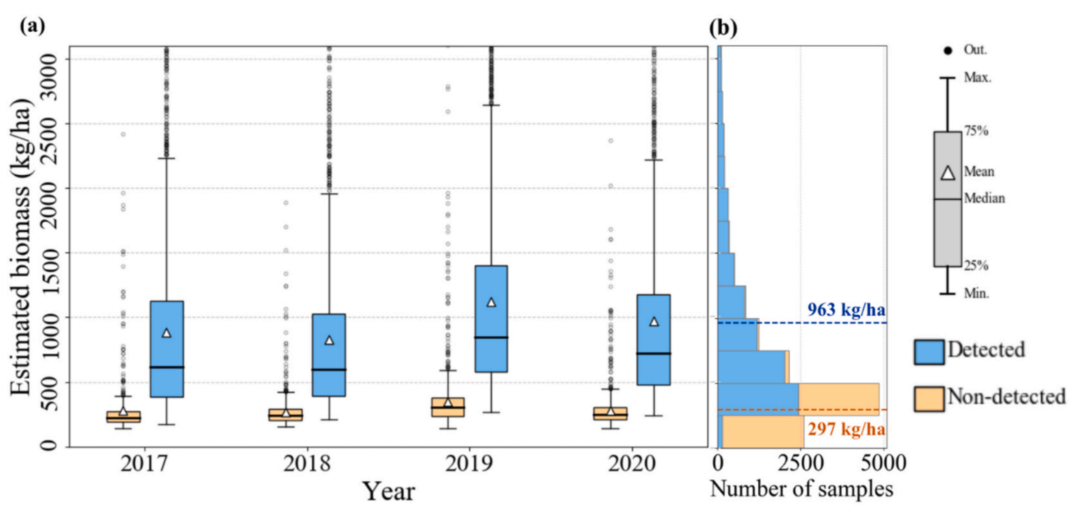

Fig. 7. Biomass distributions between detected and non-detected cover crops. The biomass (kg/ha) was estimated using the all-species time-integrated NDVI model. Panel (a) shows the statewide biomass distribution by year for detected and non-detected cover crops. Panel (b) illustrates the share of detected and non-detected cover crops across biomass intervals. The blue and orange dashed lines show the mean biomass value for detected and non-detected cover crops, respectively. The vertical axis of panel (b) corresponds to the y-axis of panel (a). Both panels cap at 3000 kg/ha for clarity; 1.8% of samples exceed 3000 kg/ha. (For interpretation of the references to colour in this figure legend, the reader is referred to the web version of this article.)

considered here. While species characteristics might influence detection accuracies, our results suggested that the dominant factor influencing

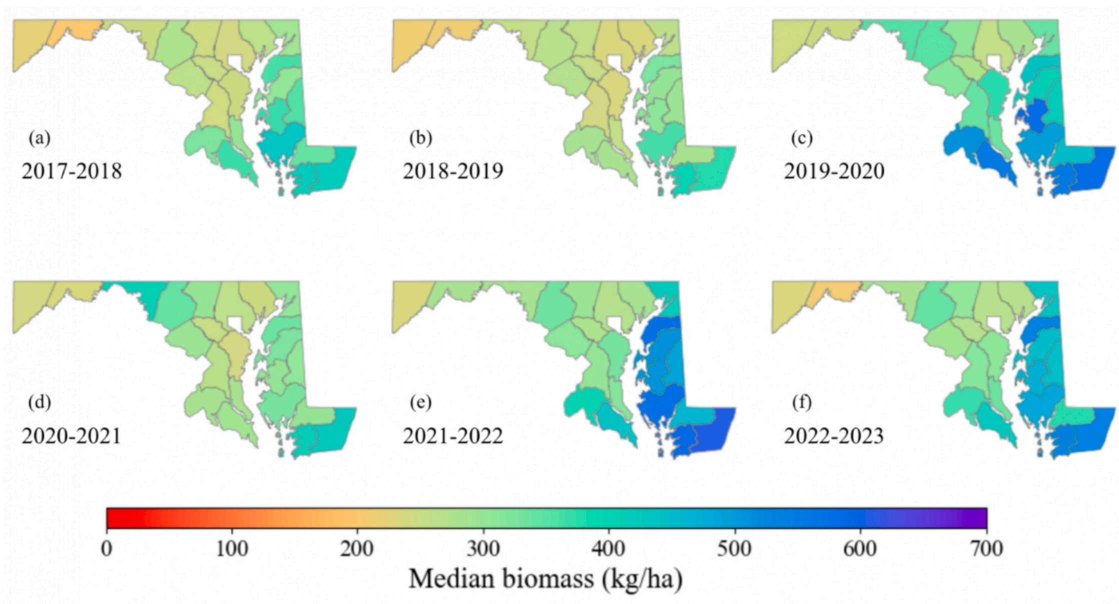

Fig. 8. Predicted winter median biomass by county. The maps show the county-level end-of-season median biomass value of all agricultural pixels that exhibit greenness features during the cover crop growing season.

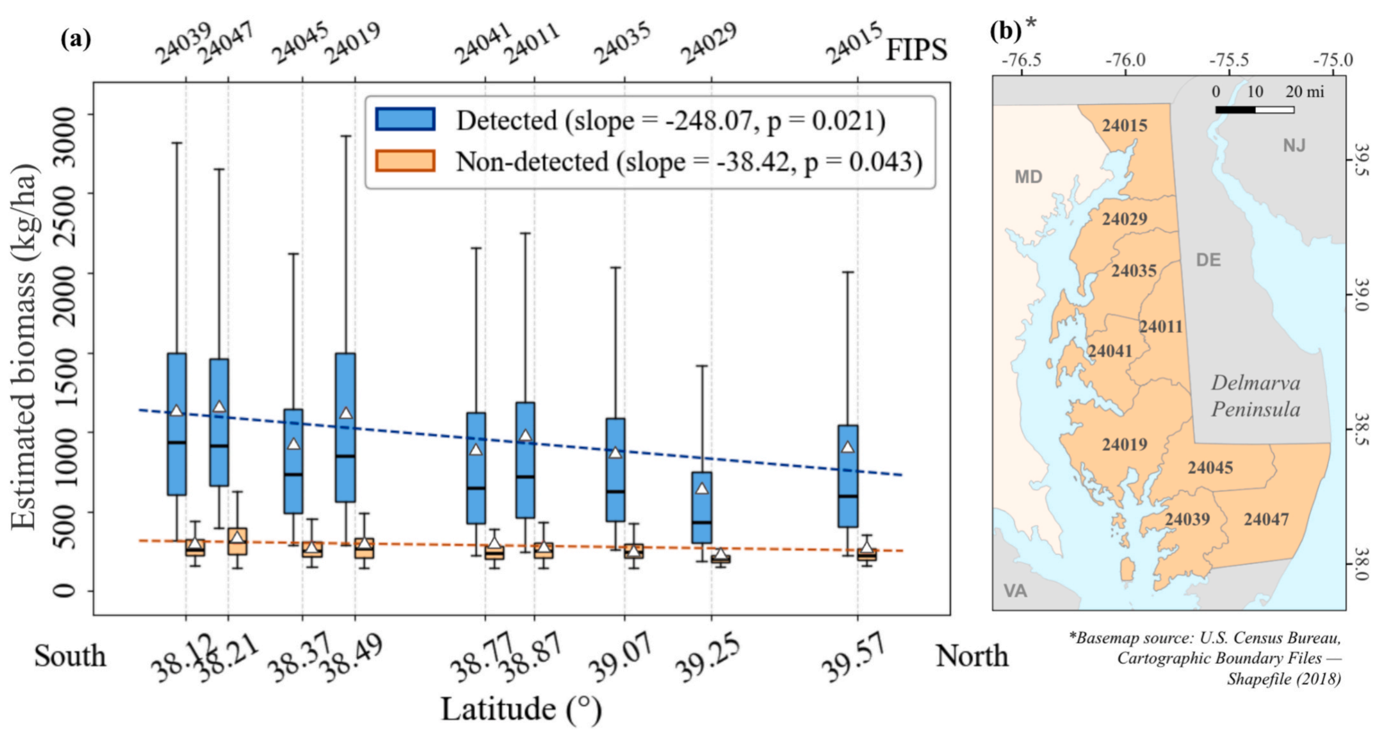

Fig. 9. Biomass distribution of Delmarva Peninsula counties. Panel (a) presents box plots of biomass distributions for detected and non-detected cover crops in each county (outliers excluded), plotted against the latitude of each county's centroid. Separate regression lines demonstrate trends in mean biomass by latitude for detected and non-detected cover crops. Panel (b) is a map of the Maryland counties on the Delmarva Peninsula, labeled by Federal Information Processing Standards (FIPS) code. Box plots in Fig. 9 share the legend with those in Fig. 7.

detection accuracy was the overall accumulated biomass.

4.3. Impact of management timing on cover crop biomass

Management timing influenced cover crop biomass because earlier planting and later termination extended the growth period and resulted in greater biomass accumulation (Fig. 11a). Longer cover crop growth periods resulted in greater accumulated GDD and further increased biomass; however, cover crop biomass remained stable after a certain amount of GDD accumulation ($R^2 = 0.88$, $p < 0.01$; a strong quadratic relationship in Fig. 11b). This relation was consistent across species (Supplementary Fig. 7). Because accumulated GDD was strongly related to growth time ($R^2 = 0.76$, $p < 0.01$; Fig. 11c), a similar quadratic relationship was observed between growth time and biomass ($R^2 = 0.57$, $p < 0.01$; Fig. 11d). Because growth time was affected by both the planting and termination dates of cover crops, the impacts of planting

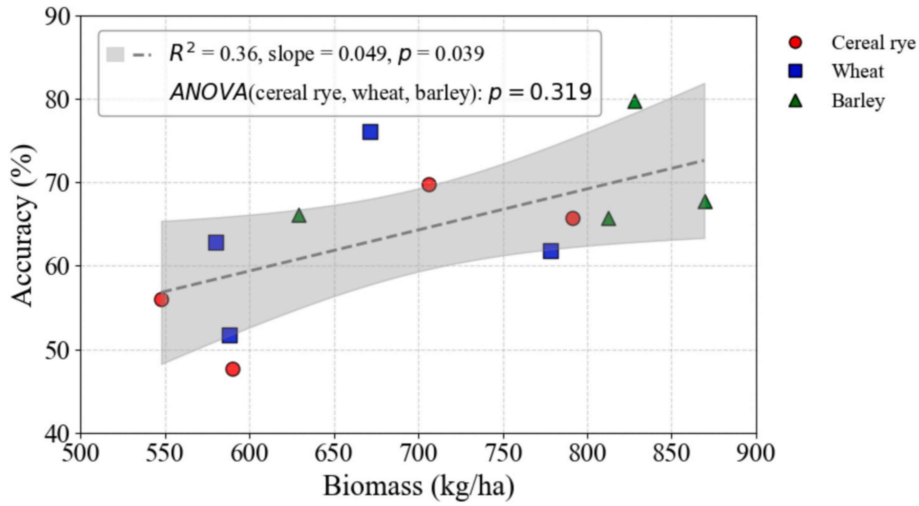

Fig. 10. Relationship between biomass and detection accuracy by dominant cover crop species across years in Maryland. Each dot represents average biomass and detection accuracy for a cover crop type planted in one season. A linear regression line captures the association between mean biomass and detection accuracy, with the gray band symbolizing the 95% confidence interval of the estimated mean accuracy prediction.

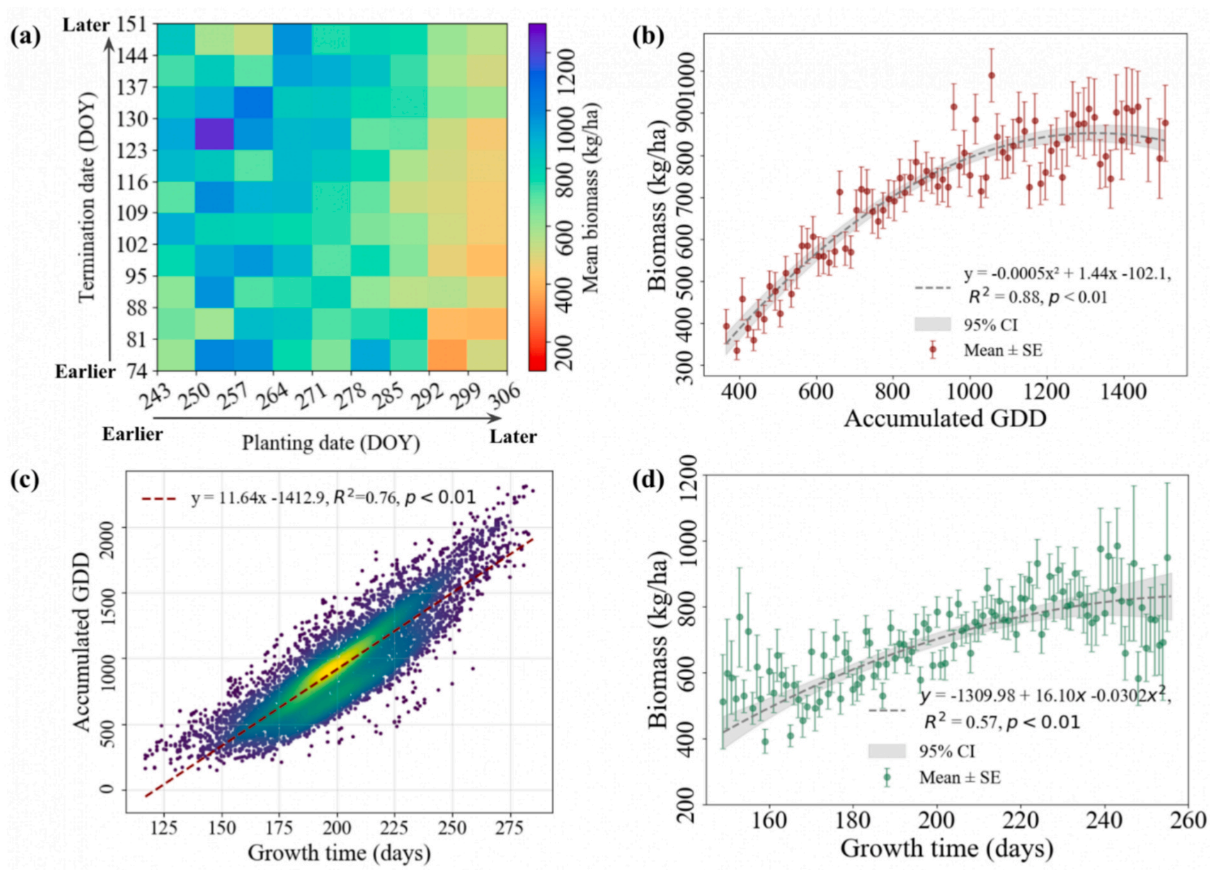

Fig. 11. Cover crop biomass by planting/termination dates (DOY), growth time, and accumulated GDD. Panel (a) shows the mean biomass, represented by color, of cover crops planted and terminated at 7-day intervals. Panel (b) shows the mean biomass under 100 bins of accumulated GDD. Panel (c) shows the relationship between growth time and accumulated GDD. Panel (d) shows the mean biomass against growth time. The bar on each dot represents the standard error of the mean.

and termination dates on cover crop biomass were examined individually. Earlier cover crop planting was generally associated with higher biomass, with peak biomass occurring for cover crops planted in early September. Biomass also increased with delayed termination, but the relationship was weaker than that between biomass and planting date (Supplementary Fig. 5).

5. Discussion

5.1. Varying performance of VIs in predicting cover crop aboveground biomass

We addressed the challenges of estimating biomass for different cover crop cereal species using satellite vegetation indices by comparing multiple VIs in single-date snapshot and time-integrated forms. The results demonstrated that NDVI outperformed NIRv and GCVI in cover crop biomass estimation. Snapshot EVI performed slightly worse than snapshot NDVI when all species were pooled, but achieved comparable results under stratified performance analysis (Supplementary Table 5). This is because NDVI, while subject to saturation at high biomass, remains reliable across the low to moderate biomass levels typical of most cover crop fields. Moreover, some studies showed NDVI had comparable prediction accuracies to other indices in estimating cover crop biomass nitrogen content (White et al., 2019), a metric highly correlated with biomass and important in evaluating the agroecosystem benefits of cover crops. We also tested the performance of some red-edge indices (Supplementary Table 6). Like previous studies, red-edge indices, such as Red-edge Ratio (RER) and Red-edge NDVI ($NDVI_{RE}$), have shown greater sensitivity to cover crop biomass (Goffart et al., 2021). However, HLS L30 product does not carry the red-edge band. It is preferable to leverage the red-edge band for biomass estimation if available in satellite data. Additionally, integrating SAR data may improve the performance by increasing the number of observations under cloudy conditions.

The time-integrated VI features served as surrogates for primary production (Yang et al., 1998) and were more accurate than the snapshot VI models. Moreover, the reduced sensitivity of time-integrated models to cover crop species was likely due to multiple factors. First, removing the soil baseline from the index minimized background influences that might contain species-related information. Second, time-integrated vegetation indices were not confined to the -1 to 1 range of the snapshot index and were thus better able to capture differences at moderate to high biomass. In contrast, snapshot VI models required calibration across species (White et al., 2019). Because NDVI uses spectral bands available on most satellite sensors, its time-integrated form can be widely utilized for cover crop biomass estimation across time, space, and species.

Machine learning (ML) models can capture complex nonlinear relationships of cover crop biomass, but we primarily used regression models in this study due to their interpretability. The time-integrated vegetation index was designed to represent cumulative plant development. Under such conditions, regression models provided a transparent mapping between predictors and biomass. We additionally implemented a random forest model using Sentinel-2 reflectance bands, NDVI, soil variables, and accumulated growing degree days. The results (Supplementary Fig. 4) showed that while the ML model improved prediction accuracy, the important predictors remained consistent with those identified in the regression framework.

Further research is needed to assess the scalability and generalizability of our cover crop biomass modeling approach. Our biomass model was calibrated using cereal cover crops common to Maryland, but broader species groups such as brassicas, legumes, and multi-species mixes were not included. A recent study that integrated proximal and satellite sensors to develop a "global" cover crop biomass model reported reduced accuracy compared to region-specific models (Jennewein et al., 2025), highlighting the importance of regional calibration and local datasets. Although our time-integrated models showed limited species sensitivity, expanding validation across diverse species and environments is necessary to improve transferability.

5.2. Integrating biomass estimation into the cover crop detection framework

The cover crop detection method in this study built on previous cover crop identification approaches. Both OpTIS (Hagen et al., 2020) and Zhou et al. (2022) used similar phenology-based frameworks that used time series of vegetation indices to identify cover crop features and set thresholds to differentiate cover crops from weeds. Extending the framework established by Zhou et al. (2022), which focused on spring-season cover crop growth, we incorporated a fall-through-spring feature that captured the full growing period and enabled the estimation of county-level thresholds. The change allowed the framework to adapt to regional variations and diverse cover crop growing scenarios, including winter-kill cover crops. In addition to these changes, we integrated biomass models into the detection framework and found that higher-biomass cover crops were more readily identified by remote sensing. Cover crop species was evaluated as a potential factor affecting detectability, and our results showed that the correlation between high detectability and high biomass held regardless of the cereal grain species. This relationship between cover crop biomass and detectability was consistent with the physical mechanism underlying vegetation indices: a higher vegetation index implied stronger phenology traits, including higher greenness content and larger leaf area, which were easier to detect by satellite. Our approach enhanced spatial specificity and cover crop phenological completeness while emphasizing that low-biomass cover crops remain challenging to detect, regardless of species or algorithm.

Cover crops with biomass above 361 kg/ha were more likely to be detected, but the detection could be influenced by multiple factors. First, cover crop species and their growing conditions determine cover crop growth. High-biomass species, favorable environmental conditions, and better management strategies (section 5.3) could make cover crops easier to detect because their vegetation signals stood out from background noise and grass. Improving the differentiation of cover crops from grass can enable our framework to detect cover crops with lower biomass. Second, differentiating overwintering crops from cover crops remained challenging, and improving overwintering crop detection can enhance our cover crop detection performance. We used CDL to remove overwintering crops (e.g., winter wheat), which could not be identified accurately in some regions. Thus, we attempted to use the termination date d_2 derived from the NDVI time series to differentiate overwintering crops from cover crops. Overwintering crops are generally harvested in late June or July in our study region, but cover crops are terminated before cash crop planting in late spring. Analysis of 174,606 winter wheat pixels in CDL from 2017 to 2022 showed substantial overlap in d_2 distributions between winter wheat and cover crops (Supplementary Fig. 9). However, d_2 alone could not differentiate between cover crops and winter wheat accurately; additional studies to further distinguish cover crops from overwintering crops are needed. Third, higher spatial and temporal resolution sensors or integration of multiple sensor sources can better capture within-field variability and subtle phenological differences, improving the accuracies of biomass estimation and the discrimination of cover crops from weeds or overwintering crops. Finally, advances in detection methods, including deep learning and computer vision approaches, may further enhance detection accuracy by capturing complex spatial and temporal patterns beyond traditional index-based methods. Together, these factors highlight that more accurate cover crop detection and biomass estimation require the integration of information on growth conditions, phenology, sensor capabilities, and analytical approaches.

5.3. Impact of cover crop management practices on biomass and its implications for incentives

Cover crop farming decisions can lead to variation in growth time that influences biomass, and incentives can have a positive impact on cover crop biomass. Earlier planting and later termination extended the growth period and allow cover crops to reach higher AccGDD, which was associated with higher biomass, aligning with the findings of previous studies (Ruis et al., 2020; Thieme et al., 2023). Since 2019, MDA has introduced late termination incentives (Thieme et al., 2023). As a result, a biomass surge was observed in 2019–2020, 2021–2022, and 2022–2023, especially for counties on the Delmarva Peninsula (Fig. 7). The 2020–2021 season did not see a similar increase, likely due to climate and pandemic disruptions.

Incentives are typically aligned with agronomic practices that maximize biomass while balancing any trade-offs with cash crop production. The MDA general incentives encourage farmers to plant earlier and terminate later, such that cover crops can accumulate sufficient biomass to reduce nitrogen leaching to groundwater (Thieme et al., 2023) or to affect weed control and nutrient availability in the cropping system (Van Eerd et al., 2023). However, excessively delayed cover crop termination may reduce cash crop yield by immobilizing nitrogen (Abdalla et al., 2019; Qin et al., 2021; Lobell et al., 2025; Muniz et al., 2025). Therefore, prioritizing earlier planting is more strategic for biomass gains when incentive funding is limited. Recent MDA programs demonstrate this balance by favoring early planting over delayed termination (Maryland Department of Agriculture, 2024; 2025). In general, cover crop management practices may be tailored to regional conditions and cover crop species to achieve biomass levels that deliver the targeted environmental benefits. In addition to management practices, environmental variables such as soil and climate should be considered in future studies of cover crop biomass.

6. Conclusion

This study examined the influence of cover crop biomass on its detectability via satellite remote sensing to inform effective cover crop management strategies. We first modeled cover crop biomass using various VIs in their single-date snapshot and time-integrated forms. Across all snapshot VIs we tested, NDVI most accurately predicted cover crop biomass compared with EVI, NIRv, and GCVI. The time-integrated NDVI model was a more accurate and consistent method for biomass estimation and significantly reduced interspecies differences. Next, we used the phenology-based framework to detect cover crops in Maryland from 2017–2018 to 2023–2024 and analyzed the impact of biomass on detectability. Higher biomass cover crops were more likely to be detected. For cover crops with biomass over 500 kg/ha, the no-buffer detection accuracy reached 96.1%, compared to an overall accuracy of 62.7% for all cover crops. Cover crop detectability was high when biomass was high, regardless of species. Finally, we found that management timing of cover crop planting/termination dates influenced cover crop biomass by altering growth duration and accumulated GDD, with biomass increasing as growth periods lengthened but plateauing after a certain level of GDD accumulation. Overall, the study provides a non-destructive, scalable approach to detect and estimate biomass across cover crop systems. This approach could help advance remote sensing applications in cover crop monitoring, support data-driven decision-making, and inform sustainable cover crop management.

CRediT authorship contribution statement

Yide Xu: Writing – review & editing, Writing – original draft, Visualization, Validation, Methodology, Investigation, Formal analysis, Conceptualization. **Qu Zhou:** Writing – review & editing, Methodology, Formal analysis, Data curation, Conceptualization. **Kaiyu Guan:** Writing – review & editing, Supervision, Resources, Funding acquisition, Data curation, Conceptualization. **Sheng Wang:** Writing – review & editing, Conceptualization. **W. Dean Hively:** Writing – review & editing, Resources, Funding acquisition. **Jyoti Jennewein:** Writing – review & editing, Data curation. **Alison Thieme:** Writing – review & editing. **Steven Mirsky:** Writing – review & editing, Data curation. **Zhangliang Chen:** Writing – review & editing, Project administration.

Declaration of competing interest

The authors declare that they have no known competing financial interests or personal relationships that could have appeared to influence the work reported in this paper.

Acknowledgments

This work was primarily supported by USDA National Institute of Food and Agriculture (NIFA) Foundational Program awards (2017-67013-26253, 2017-68002-26789, 2017-67003-28703, 2022-68013-37052), NASA Acres Consortium, USDA Economic Research Service (ERS), USDA Office of Chief Economist, US Department of Energy's Advanced Research Projects Agency-Energy (ARPA-E) SMARTFARM (MBC Lab and SYMFONI) projects, and NSF CAREER Award by Environmental Sustainability Program. This work was also supported in part by the C3. ai Digital Transformation Institute. K.G. and Q.Z. acknowledge the support from the NASA FINESST award. S.W. is supported by the NASA Early Career Investigator Program in Earth Science (80NSSC24K1057). W.D.H. acknowledges the support of the USGS National Land Imaging Program and the USDA Long Term Agricultural Research network. This work is also partially funded by Foundation for Food & Agriculture Research (FFAR) Seeding Solutions Award (Grant 602757). The views and conclusions in this article represent the views solely of the authors and do not represent the views of the above U.S. government agencies except the U.S. Geological Survey. Any use of trade, firm, or product names is for descriptive purposes only and does not imply endorsement by the U.S. Government.

Appendix A. Supplementary data

Supplementary data to this article can be found online at https://doi.org/10.1016/j.jag.2026.105453.

Data availability

Contact the corresponding author to request cover crop data for Maryland. All other input data can be acquired from the sources as noted in the manuscript.

References

Abdalla, M., Hastings, A., Cheng, K., Yue, Q., Chadwick, D., Espenberg, M., Truu, J., Rees, R.M., Smith, P., 2019. A critical review of the impacts of cover crops on nitrogen leaching, net greenhouse gas balance and crop productivity. Glob. Chang. Biol. 25 (8), 2530–2543. https://doi.org/10.1111/gcb.14644.

Abernethy, J., Beeson, P., Boryan, C., Hunt, K., Sartore, L., 2023. Preseason crop type prediction using crop sequence boundaries. Comput. Electron. Agric. 208, 107768. https://doi.org/10.1016/j.compag.2023.107768.

Ahmed, Z., Nalley, L., Brye, K., Steven Green, V., Popp, M., Shew, A.M., Connor, L., 2023. Winter-time cover crop identification: a remote sensing-based methodological framework for new and rapid data generation. Int. J. Appl. Earth Obs. Geoinf. 125, 103564. https://doi.org/10.1016/j.jag.2023.103564.

Badgley, G., Field, C.B., Berry, J.A., 2017. Canopy near-infrared reflectance and terrestrial photosynthesis. Sci. Adv. 3 (3), e1602244. https://doi.org/10.1126/sciadv.1602244.

Blanco-Canqui, H., 2022. Cover crops and carbon sequestration: Lessons from U.S. studies. Soil Sci. Soc. Am. J. 86 (3), 501–519. https://doi.org/10.1002/saj2.20378.

Boryan, C., Yang, Z., Mueller, R., Craig, M., 2011. Monitoring US agriculture: the US Department of Agriculture, National Agricultural Statistics Service. Cropland Data Layer Program. Geocarto International 26 (5), 341–358. https://doi.org/10.1080/10106049.2011.562309.

Cai, T., Chang, C., Zhao, Y., Wang, X., Yang, J., Dou, P., Otgonbayar, M., Zhang, G., Zeng, Y., Wang, J., 2024. Within-season estimates of 10 m aboveground biomass based on Landsat, Sentinel-2 and PlanetScope data. Sci. Data 11 (1), 1276. https://doi.org/10.1038/s41597-024-04120-3.

Chen, K., 2025. High-resolution Winter Cover Crop Mapping with PlanetScope Imagery: Comparative Analysis of Random Forest, Convolutional Neural Network, and Unsupervised Classification. Sci. Remote Sens. 100351. https://doi.org/10.1016/j.srs.2025.100351.

Claverie, M., Ju, J., Masek, J.G., Dungan, J.L., Vermote, E.F., Roger, J.-C., Skakun, S.V., Justice, C., 2018. The Harmonized Landsat and Sentinel-2 surface reflectance data set. Remote Sens. Environ. 219, 145–161. https://doi.org/10.1016/j.rse.2018.09.002.

Delgado, J.A., Barrera Mosquera, V.H., Alwang, J.R., Villacis-Aveiga, A., Cartagena Ayala, Neer, D., Monar, C., Escudero López, L.O., 2021. Potential Use of Cover Crops for Soil and Water Conservation, Nutrient Management, and Climate Change Adaptation across the Tropics. Adv. Agronom. 165, 175–247. https://doi.org/10.1016/bs.agron.2020.09.003.

Fan, H., Liu, S., Li, J., Li, L., Dang, L., Ren, T., Lu, J., 2021. Early prediction of the seed yield in winter oilseed rape based on the near-infrared reflectance of vegetation

(NIRv). Comput. Electron. Agric. 186, 106166. https://doi.org/10.1016/j.compag.2021.106166.

Fowler, D.B., Byrns, B.M., Greer, K.J., 2014. Overwinter Low-Temperature responses of Cereals: analyses and simulation. Crop Sci. 54 (6), 2395–2405. https://doi.org/10.2135/cropsci2014.03.0196.

Gao, F., Jennewein, J., Hively, W.D., Soroka, A., Thieme, A., Bradley, D., Keppler, J., Mirsky, S., Akumaga, U., 2023. Near real-time detection of winter cover crop termination using harmonized Landsat and Sentinel-2 (HLS) to support ecosystem assessment. Sci. Remote Sens. 7, 100073. https://doi.org/10.1016/j.srs.2022.100073.

Gerhards, R., Schappert, A., 2020. Advancing cover cropping in temperate integrated weed management. Pest Manag. Sci. 76 (1), 42–46. https://doi.org/10.1002/ps.5639.

Gitelson, A.A., Viña, A., Arkebauer, T.J., Rundquist, D.C., Keydan, G., Leavitt, B., 2003. Remote estimation of leaf area index and green leaf biomass in maize canopies. Geophys. Res. Lett. 30 (5), 2002GL016450. https://doi.org/10.1029/2002GL016450.

Goffart, D., Curnel, Y., Planchon, V., Goffart, J.-P., Defourny, P., 2021. Field-scale assessment of Belgian winter cover crops biomass based on Sentinel-2 data. Eur. J. Agron. 126, 126278. https://doi.org/10.1016/j.eja.2021.126278.

Hagen, S.C., Delgado, G., Ingraham, P., Cooke, I., Emery, R., Fisk, P., J., Melendy, L., Olson, T., Patti, S., Rubin, N., Ziniti, B., Chen, H., Salas, W., Elias, P., & Gustafson, D., 2020. Mapping Conservation Management Practices and Outcomes in the Corn Belt using the Operational Tillage Information System (OpTIS) and the Denitrification–Decomposition (DNDC) Model. Land 9 (11), 408. https://doi.org/10.3390/land9110408.

Hively, W.D., Gao, F., McCarty, G.W., Daughtry, C.S.T., Zhang, X., Jennewein, J., Thieme, A., Lamb, B.T., Keppler, J., Hapeman, C.J., Cosh, M., Mirsky, S.B., 2025. Satellite Assessment of Winter Cover Crop and Conservation Tillage Outcomes to support Adaptive Management in Working Landscapes. J. Environ. Qual. 2025 (54), 1548–1571. https://doi.org/10.1002/jeq2.70082.

Hu, Q., Thomas, B.W., Powlson, D., Hu, Y., Zhang, Y., Jun, X., Shi, X., Zhang, Y., 2023. Soil organic carbon fractions in response to soil, environmental and agronomic factors under cover cropping systems: a global meta-analysis. Agr. Ecosyst. Environ. 355, 108591. https://doi.org/10.1016/j.agee.2023.108591.

Huete, A., Didan, K., Miura, T., Rodriguez, E.P., Gao, X., Ferreira, L.G., 2002. Overview of the radiometric and biophysical performance of the MODIS vegetation indices. Remote Sens. Environ. 83 (1–2), 195–213. https://doi.org/10.1016/S0034-4257(02)00096-2.

Jennewein, J.D., Hively, W.D., Thieme, A., Lamb, B., Mirsky, S., 2022. *Winter cover crop biomass sampling at the Beltsville Agricultural Research Center, 2019-2021, with corresponding Sentinel-1 and Sentinel-2 derived indices and metrics*. Geological Survey, U.S. https://doi.org/10.5066/P9ASSF1T.

Jennewein, J.S., Davis, B.W., Seehaver-Eagen, S., Nicolette, J., Pittman, J., Hively, W.D., Mirsky, S.B., 2025. Multi-sensor proximal remote sensing for cover crop biomass estimation at high and moderate spatial resolutions. Smart Agric. Technol., 101201 https://doi.org/10.1016/j.atech.2025.101201.

Kumar, V., Singh, V., Flessner, M.L., Reiter, M.S., Kumari, A., Price, A., Kuhar, T.P., Mirsky, S.B., 2025. Impact of cover crops and termination timing on weed management in corn. Weed Technol 39, e69. https://doi.org/10.1017/wet.2025.39.

Liu, W., Xu, C., Zhang, Z., De Boeck, H., Wang, Y., Zhang, L., Xu, X., Zhang, C., Chen, G., Xu, C., 2023. Machine learning-based grassland aboveground biomass estimation and its response to climate variation in Southwest China. Front. Ecol. Evol. 11, 1146850. https://doi.org/10.3389/fevo.2023.1146850.

Lobell, D.B., Di Tommaso, S., Zhou, Q., Ma, Y., Specht, J., Guan, K., 2025. The mixed effects of recent cover crop adoption on US cropland productivity. Nat. Sustain. https://doi.org/10.1038/s41893-025-01599-5.

Maryland Department of Agriculture. (2024). 2024/2025 Winter Cover Crop Program Requirements and Agreement, accessed November 1, 2025 at https://mda.maryland.gov/resource_conservation/counties/FY25-CoverCrop-Agreement-Requirements.pdf.

Maryland Department of Agriculture. (2025). 2025/2026 Winter Cover Crop Program Requirements and Agreement, accessed November 1, 2025 at https://mda.maryland.gov/resource_conservation/counties/FY26_Program_Requirements_and_Agreement.pdf.

Mirsky, S.B., Ryan, M.R., Teasdale, J.R., Curran, W.S., Reberg-Horton, C.S., Spargo, J.T., Wells, M.S., Keene, C.L., Moyer, J.W., 2013. Overcoming Weed Management challenges in Cover Crop–Based Organic Rotational No-till soybean production in the Eastern United States. Weed Technol. 27 (1), 193–203. https://doi.org/10.1614/WT-D-12-00078.1.

Muniz, C.R., Silva, T.S., Ferreira, C.J.B., Conley, S., Mourtzinis, S., McClure, J., Naeve, S., Vann, R., De Freitas Souza, M., 2025. How changes in cover crop termination timing affect soybean yield? a systematic review and meta-analysis. Field Crops Res. 326, 109876. https://doi.org/10.1016/j.fcr.2025.109876.

Prabhakara, K., Hively, W.D., McCarty, G.W., 2015. Evaluating the relationship between biomass, percent groundcover and remote sensing indices across six winter cover crop fields in Maryland, United States. Int. J. Appl. Earth Observ. Geoinform. 39, 88–102. https://doi.org/10.1016/j.jag.2015.03.002.

PRISM Climate Group, 2022. PRISM gridded climate data. Retrieved from. https://prism.oregonstate.edu.

Qin, Z., Guan, K., Zhou, W., Peng, B., Villamil, M.B., Jin, Z., Tang, J., Grant, R., Gentry, L., Margenot, A.J., Bollero, G., Li, Z., 2021. Assessing the impacts of cover crops on maize and soybean yield in the U.S. midwestern agroecosystems. Field Crops Res. 273, 108264. https://doi.org/10.1016/j.fcr.2021.108264.

Ruis, S.J., Blanco-Canqui, H., Elmore, R.W., Proctor, C., Koehler-Cole, K., Ferguson, R.B., Francis, C.A., Shapiro, C.A., 2020. Impacts of cover crop planting dates on soils after four years. Agronom. J. 112 (3), 1649–1665. https://doi.org/10.1002/agj2.20143.

Servia, H., Pareeth, S., Michailovsky, C.I., De Fraiture, C., Karimi, P., 2022. Operational framework to predict field level crop biomass using remote sensing and data driven models. Int. J. Appl. Earth Observ. Geoinform. 108, 102725. https://doi.org/10.1016/j.jag.2022.102725.

Shammi, S.A., Meng, Q., 2021. Use time series NDVI and EVI to develop dynamic crop growth metrics for yield modeling. Ecological Indicators 121, 107124. https://doi.org/10.1016/j.ecolind.2020.107124.

Shuai, G., Fowler, A., Basso, B., 2024. Within-season vegetation indices and yield stability as a predictor of spatial patterns of Maize (*Zea mays* L) yields. Precis. Agric. 25 (2), 963–982. https://doi.org/10.1007/s11119-023-10101-0.

Soil Survey Staff, 2020. *Gridded Soil Survey Geographic (gSSURGO) Database for Maryland*. USDA, NRCS. Available online at https://gdg.sc.egov.usda.gov/.

Thieme, A., Hively, W.D., Gao, F., Jennewein, J., Mirsky, S., Soroka, A., Keppler, J., Bradley, D., Skakun, S., McCarty, G.W., 2023. Remote sensing evaluation of winter cover crop springtime performance and the impact of delayed termination. Agronom. J. 115 (1), 442–458. https://doi.org/10.1002/agj2.21207.

USDA NASS. (2017-2022). Quick Stats. Retrieved October 15, 2024 from https://quickstats.nass.usda.gov.

Van Eerd, L.L., Chahal, I., Peng, Y., Awrey, J.C., 2023. Influence of cover crops at the four spheres: a review of ecosystem services, potential barriers, and future directions for North America. Sci. Total Environ. 858, 159990. https://doi.org/10.1016/j.scitotenv.2022.159990.

White, C.M., Bradley, B., Finney, D.M., Kaye, J.P., 2019. Predicting Cover Crop Nitrogen Content with a Handheld Normalized Difference Vegetation Index Meter. Agricult. Environ. Lett. 4 (1), 190031. https://doi.org/10.2134/ael2019.08.0031.

Yang, L., Wylie, B.K., Tieszen, L.L., Reed, B.C., 1998. An analysis of relationships among climate forcing and time-integrated NDVI of grasslands over the US northern and central Great Plains. Remote Sens. Environ. 65 (1), 25–37. https://doi.org/10.1016/S0034-4257(98)00012-1.

Zhou, Q., Guan, K., Wang, S., Jiang, C., Huang, Y., Peng, B., Chen, Z., Wang, S., Hipple, J., Schaefer, D., Qin, Z., Stroebel, S., Coppess, J., Khanna, M., Cai, Y., 2022. Recent Rapid increase of Cover Crop Adoption across the U.S. Midwest Detected by Fusing Multi-Source Satellite Data. Geophys. Res. Lett. 49 (22), e2022GL100249. https://doi.org/10.1029/2022GL100249.

Zhou, Q., Guan, K., Wang, S., Wu, X., Stroebel, S., Hipple, J., 2026. Multi-sensor assessment of phenology-based field-level cover cropping detection using satellite vegetation time series from Harmonized Landsat-8 and Sentinel-2, MODIS, and PlanetScope. Int. J. Appl. Earth Observ. Geoinform. 146, 105004. https://doi.org/10.1016/j.jag.2025.105004.